Molecular BioSystems

Accepted Manuscript

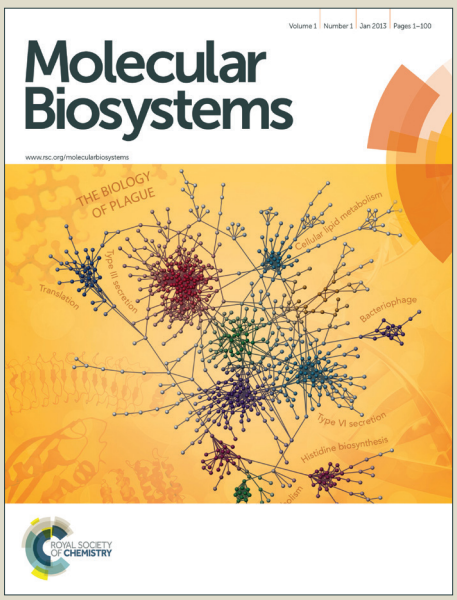

ROYAL SOCIETY OF CHEMISTRY

www.rsc.org/molecularbiosystems

Proteomic and metabolic profile of Cakile maritima Scop. Sea Rocket grown in the presence of Cadmium

Manel Taamalli[2#], Angelo D'Alessandro[1#], Cristina Marrocco[1], Federica Gevi[1], AnnaMaria Timperio[1], Lello Zolla[1]*

1 Department of Ecological and Biological Sciences, University of Tuscia, Largo dell'Università, snc, 01100 Viterbo, Italy

2 Laboratoire des Plantes Extrêmophiles, Centre de Biotechnologie de Borj-Cédria, BP 901, 2050 Hammam-lif, Tunisia

This authors sharing the first authorship

* **Corresponding Authors**:

* Prof. Lello Zolla - Tuscia University, Largo dell'Università snc, 01100 Viterbo, Italy. Tel.: +39 0761 357 100; fax: +39 0761 357 179. E-mail address: zolla@unitus.it (L. Zolla)

Running title: **Cadmium stress responses in Cakile maritima Scop. Sea Rocket**

Keywords: *Cakile maritima Scop. Sea Rocket*; proteomics; metabolomics; phytoremediation; abiotic stress.

Abstract

Recent physiological reports have documented how *Cakile maritima Scop. Sea Rocket* could accumulate high doses of Cd without altering its physiological parameters. In the present study, we performed an integrated proteomics (2DE) and metabolomics (HPLC-MS) investigation to determine the molecular mechanisms underlying cadmium (Cd) tolerance of this halophyte. Peculiar features were observed: i) up-regulation of thiol compound anabolism, including glutathione and phytochelatin homeostasis, which allows an intracellular chelation of Cd and its compartmentalization into vacuole by a significant up-regulation of vacuolar transporters; ii) up-regulation of the PPP and Calvin cycle (both at the enzyme and metabolite level), which utterly promoted the maintenance of NADPH/$NADP^+$ homeostasis, other than the accumulation of triose-phosphates (serving as anabolic intermediates for triacylglycerol biosynthesis) and the glyoxylate precursor phosphoglycolate, to promote photorespiration and consequently CO_2 release. A up-regulation of carbonic anhydrase was also observed.

This halophyte is also correlated with a high efficient antioxidant system, especially a high up-regulation of SOD1, resulting more efficient in coping with heavy metals stress than common plants. Interestingly, exposure to high Cd concentrations partly affected photosystem integrity and metabolic activity, through the up-regulation of enzymes from the Calvin cycle and glutathione-ascorbate homeostasis and PAP3 which stabilizes thylakoid membrane structures. In addition, up-regulation of Peptidyl-prolyl isomerase CYP38 increases stability and biogenesis of PSII.

Finally, metabolomics results confirmed proteomics and previous physiological evidence, also suggesting that osmoprotectants betaine and proline, together with plant hormones methyl jasmonate and salicylic acid might be involved in mediating responses to Cd-induced stress.

Taken together, these peculiar features confirm that *Cakile maritima Scop. Sea Rocket* seemed to be naturally equipped to withstand even high doses of Cd pollution.

1. Introduction

Some anthropogenic activities (viz mining, the use of chemical fertilizers or metal-based pesticides, industrial activities) have been increasingly associated with the introduction of toxic heavy metal compounds into the environment.[1] Cadmium (Cd), one of the most potentially harmful heavy metals[2], contaminates air and soils exposed to heavy traffic and industrial wastes, and thus enters the food chain via plant contamination[3].

However, plant capacity to extract heavy metals from the soil has been recently proposed as a viable strategy to cope with heavy metal soil contamination, through a process that goes by the name of phytoremediation. Phytoremediation is based on the assumption that while certain plants can resist to heavy metal exposure by avoiding their uptake from the soil, others can actually promote the uptake of heavy metals and their compartmentalization in the aerial parts, which would ease the decontamination of the soil through the systematic harvest of contaminated plants[4]. While *Brassicaceae* have long been identified as heavy metal hyperaccumulators and still represent a key model for molecular investigations in the field of phytoremediation, "omics"[5] and physiological studies have progressively unveiled that exposure of *Brassicaceae* to heavy metal stress (Cd in particular[6–9]) can induce severe disturbances in the plant physiological homeostasis, as they impair photosynthesis, water use efficiency, mineral uptake (especially divalent ions) and photosynthetic electron transport[6–9]. At the same time, Cd exposure promotes leaf chlorosis, premature senescence of chloroplast, stomatal closure, carbon assimilation and, utterly, growth retardation[6–9]. These events are further exacerbated by Cd-induced accumulation of reactive oxygen species (ROS) and oxidative stress, which promotes radical-induced protein fragmentation and destabilization of key energy-metabolism and photosynthesis-related multiprotein complexes[10]. In the light of the pleiotropic harmful effects triggered by Cd accumulation in *Brassicaceae*, one key goal in the agenda of researchers involved in the study of phytoremediation biology is the individuation of the most valid plant species that could better cope with Cd exposure without compromising the metal hyperaccumulation behavior. In this view, halophytic plants are increasingly emerging as valid candidates[11]. Recent physiological investigations on *Cakile maritima Scop. Sea Rocket* and *Brassica juncea Czern* responses to Cd stress[12] highlighted that the former could accumulate almost twice the dose of Cd in shoots in comparison to the latter. Cd tolerance was also higher in *Cakile maritima Scop. Sea Rocket* than in *Brassica juncea Czern*, since the former could also better tolerate it since mild or heavy Cd stress did not alter physiological parameters, including mineral uptake, pigment content, intracellular CO_2, quantum efficiency of photosystem II (PSII) and photosystem efficiency related parameters[21]. On the other hand, minor alterations were observed only upon exposure to high doses (100 μM) of $CdCl_2$ in terms of growth retardation (-30% in comparison to >60% in *Brassica juncea Czern*), transpiration, stomatal conductance, water use efficiency and non-photochemical quenching of chlorophyll fluorescence and variation of net CO_2 assimilation, suggesting that elevated doses of Cd might result in minor deregulations of photoprotective mechanisms and photorespiration[12]. The results reported by Taamalli et al.[12] indicate that the halophyte *Cakile maritima Scop. Sea Rocket* can tolerate even high doses of Cd and accumulates it not only in the roots, as observed in *Brassica juncea Czern*, but it also promotes a concentration dependent translocation of Cd in the shoots, without substantially disrupting the plant physiological balance, which makes it a suitable candidate for phytoremediation interventions in Cd-contaminated soils[12].

Of note that halophytic plants are naturally present in environments characterized by an excess of toxic ions (especially sodium and chloride), though they can also tolerate other stresses including heavy metals owing to shared physiological mechanisms of salt and heavy metal stress resistance[11]. Indeed, two main mechanisms underlie halophytic plants capacity to cope with saline environments, analogously to plant responses to heavy metal stress, that is to say salt tolerance (salt accumulators) and salt avoidance, where the plants do not allow the penetration of salt ions into their

sensitive cells[11]. One clear advantage of halophytic phytoaccumulators over "classic" ones is that they can often tolerate extreme environmental conditions, including elevated salinity, drought and heat, all these features coming in handy when trying to remediate soils whereby saline water is the only available option to irrigate, and drought and heat might be an issue (such as in the case of arid regions, whereby the quality of irrigation waters is decreasing as water supplies for agriculture become restricted due to urban needs and climate change). In addition, irrigation with saline waters would reduce heavy metal soil sorption and promote heavy metal bioavailability and translocation from the roots to the aerial parts[13,14].

In the light of this encouraging body of literature, in the present study we decided to apply an integrated proteomics and metabolomics analytical workflow to complement physiological information on the biological responses of a halophyte plant, *Cakile maritima Scop. Sea Rocket,* to Cd exposure[12]. Of note, the present study showed that Cd tolerance in *Cakile maritima Scop. Sea Rocket* partly relies on the very same molecular mechanisms that are activated by salt stress[15,16,17] while we hereby also highlighted the up-regulation of thiol compound anabolism, including glutathione and phytochelatin homeostasis, especially in response to elevated Cd stress (100 μM). Moreover, altered energy metabolism at the triose phosphate level was accompanied by altered accumulation of Calvin cycle intermediates and photorespiration byproducts, conversely to what we recently reported for the less tolerant *Brassica juncea*[5]. Finally, metabolomics results confirmed proteomics and physiological evidence, also suggesting that osmoprotectants betaine and proline, together with plant hormones methyl jasmonate and salicylic acid might be involved in mediating responses to Cd-induced stress.

Materials and Methods

Plant growth condition and Cd treatment

Plants were kindly provided by Prof. T. Ghanaya. On the same physiological investigations were performed and published elsewhere[12]. Briefly, plants were grown as follow: mature seeds of *Cakile maritima Scop. Sea Rocket* (European Sea Rocket) harvested at Raoued, a locality close to the Mediterranean seashore, 20 km north of Tunis were germinated in Petri dishes (10 cm) containing two layers of filter papers moistened with deionized water and incubated in the dark at 30°C for 4 days. The experiments were carried out in a glass house with 16 h light period at a minimal light intensity of 250 µmol m-2 s-1. Following germination, seedlings were transferred to plastic pots filled with 5L of Hoagland solution. The cultures were achieved in a greenhouse under controlled conditions, photoperiod of 16/8 h (light/darkness), daily air temperature and relative humidity ranging 25–20°C and 55–75%, respectively. Growth solutions were continuously aerated and renewed every three days. After two weeks of Cd-free growth, seedlings were randomly assigned to four different Cd treatments: 0, 25, 50 and 100 µM $CdCl_2$ for duration of 21 days. At harvest, leaves collected for proteomics and metabolomics analyses were immediately frozen in liquid nitrogen and stored at -80°C. The remaining intact plants were harvested, cut into shoots and roots, weighed, and oven-dried at 60°C for dry mass and Cd content determination.

Proteomics

Protein extraction and 2DE

Leaves both apical and basal were finely powdered in liquid nitrogen and processed further as mentioned in Fagioni et al[18]. Proteins were stained by Coomassie Brilliant Blue G-250 stain.

A total of 12 2DE gels (4 biological replicates per group – control, 25 µM and 100 µM $CdCl_2$) have been performed during the proteomic analysis.

Stained gels were digitalized, and image analysis was performed using PDQuest 2-D analysis software 1709620 (Biorad, Milan, Italy).

Spots from 2-DE maps of biological interest ($p<0.05$ ANOVA, fold-change > 1.5) were carefully excised from the gel and subjected to in-gel trypsin digestion according to Shevchenko et al.[19] with minor modifications. Protein identification was performed as previously reported[5], through a nanoHPLC (Proxeon, Bruker Daltonics, Germany) and MS/MS ion trap (Amazon ETD, Bruker Daltonics, Germany) system. Instrument settings were consistent with our previous studies[5]. In particular, the spray capillary was a fused silica capillary, 0.090mm o.d., 0.020mm i.d.. For all experiments, a sample volume of 15 µL was loaded by the autosampler onto a homemade 2 cm fused silica precolumn (100 µm I.D.; 375 µm O.D.; Reprosil C18-AQ, 5 µm, Dr. Maisch GmbH, Ammerbuch-Entringen, Germany). Sequential elution of peptides was accomplished using a flow rate of 300 nL/min and a linear gradient from Solution A (2% acetonitrile; 0.1% formic acid) to 50% of Solution B (98% acetonitrile; 0.1% formic acid) in 40 min over the precolumn in-line with a homemade 15 cm resolving column (75 µm I.D.; 375 µm O.D.; Reprosil C18-AQ, 3 µm, Dr. Maisch GmbH, Ammerbuch-Entringen, Germany). The acquisition parameters for the instrument were as follows: dry gas temperature, 220 °C; dry gas, 4.0 L/min; nebulizer gas, 10 psi; electrospray voltage, 4000 V; high-voltage end-plate offset, −200 V; capillary exit, 140 V; trap drive: 63.2; funnel 1 in, 100 V out 35 V and funnel 2 in, 12 V out 10 V; ICC target, 200000; maximum accumulation time, 50 ms. The sample was measured with the “Enhanced Resolution Mode”

at 8100 m/z per second (which allows mono isotopic resolution up to four charge stages) polarity positive, scan range from m/z 300 to 1500, 5 spectra averaged, and rolling average of 1. The "Smart Decomposition" was set to "auto".

Acquired CID spectra were processed in DataAnalysis 4.0, and deconvoluted spectra were further analyzed with BioTools 3.2 software and submitted to Mascot search program (in-house version 2.2, Matrix Science, London, UK).

The following parameters were adopted for database searches with Mascot search program: NCBInr database (release date March 10, 2013; 247209 sequences); taxonomy=Viridiplantae; peptide mass tolerance of ±0.3 Da; fragment mass tolerance of ±0.3 for CID ions, in agreement with our recent publications[5]; enzyme specificity trypsin with 2 missed cleavages considered; fixed modifications: carbamidomethyl (C); variable modifications: oxidation (M). The criterion for acceptance of a peptide assignment corresponded to an ions score ≥ the 95% confidence interval, together with the identification of at least two peptides with Mascot scores ≥ 35 each.

Metabolomics

Leaves (200 mg per group, 4 biological replicates per group – the same plants from which samples for proteomics analyses were collected) were finely ground in liquid nitrogen and powder was used for metabolomics extractions and subsequent analyses. Extraction and metabolomics analyses were performed as previously reported[20]. Briefly, leaf powder was collected in separated tubes and a volume of 0.15 ml of ice cold ultra-pure water (18 mΩ) was added. Tubes were then placed into a water bath at 37 °C for 0.5 min. Samples were mixed with 0.6 ml of -20 °C methanol and then with 0.45 ml chloroform. Subsequently, 0.15 ml of ice cold ultra-pure water were added to each tube and they were transferred to a -20 °C freezer for 2–8 h. An equivalent volume of acetonitrile was added to the tube and transferred to a refrigerator (4 °C) for 20 min. Samples with precipitated proteins were thus centrifuged at 10 000 x g for 10 min at 4 °C.

Finally, samples were dried in a rotational vacuum concentrator (RVC 2–18 – Christ Gmbh; Osterode am Harz, Germany) and re-suspended in 200 ml of water, 5% formic acid and transferred to glass auto-sampler vials for LC/MS analysis.

Rapid resolution reversed-phase HPLC. An Ultimate 3000 Rapid Resolution HPLC system (LC Packings, DIONEX, Sunnyvale, USA) was used to perform metabolite separation. The system featured a binary pump and a vacuum degasser, a well-plate autosampler with a six-port micro-switching valve, a thermostated column compartment. Samples were loaded onto a Reprosil C18 column (2.0 mm x 150 mm, 2.5 µm – Dr Maisch, Germany) for metabolite separation[20].

Chromatographic separations were achieved at a column temperature of 30 °C; and a flow rate of 0.2 ml/min.

For downstream positive ion mode (+) MS analyses, a 0–100% linear gradient of solvent A (ddH_2O, 0.1% formic acid) to B (acetonitrile, 0.1% formic acid) was employed over 30 min, returning to 100% A in 2 min and stay for 6 min post-time in solvent A [20].

Mass spectrometry: Q-TOF settings.

Mass spectrometry analysis was carried out on an electrospray hybrid quadrupole time-of flight mass spectrometer MicroTOF-Q (Bruker-Daltonik, Bremen, Germany) equipped with an ESI ion source. Mass spectra for metabolite extracted samples were acquired both in positive and in negative ion mode. ESI capillary voltage was set at 4500 V (+) ion mode. The liquid nebulizer was set to 27 psi and the nitrogen drying gas was set to a flow rate of 6 l/min. The dry gas temperature was maintained at 200 °C. Data were acquired with a stored mass range of m/z 50–1200. Automatic isolation and fragmentation (AutoMSn mode) was performed on the 4 most intense ions simultaneously throughout the whole scanning period (30 min per run) to validate metabolite identifications, although peak area quantifications were performed on intact mass spectra, as previously reported[5].

Instrument calibration was performed externally every day with a sodium formate solution consisting of 10 mM sodium hydroxide in 50% isopropanol : water, 0.1% formic acid. Automated internal mass scale calibration was performed through direct automated injection of the calibration solution at the beginning and at the end of each run by a 6-port divert-valve.

Data elaboration and statistical analysis

In order to reduce the number of possible hits in molecular formula generation, we exploited the SmartFormula3D TM software (Bruker Daltonics, Bremen, Germany), which directly calculates molecular formulae based upon the MS spectrum (isotopic patterns) and transition fingerprints (fragmentation patterns). This software generates a confidence-based list of chemical formulae on the basis of the precursor ions and all fragment ions, and the significance of their deviations to the predicted intact mass and fragmentation pattern. Triplicate runs for each one of the 4 biological replicates were exported as mzXML files and processed through MAVEN[21]. Mass spectrometry chromatograms were elaborated for peak alignment, matching and comparison of parent and fragment ions, and tentative metabolite identification (within a 20 ppm mass-deviation range between observed and expected results against the imported KEGG database[22]. MAVEN is an open-source software that could be freely downloaded from the official project websites (http://genomics-pubs.princeton.edu/mzroll/index.php?show=download). Metabolite assignment was further elaborated in the light of the hydrophobicity/hydrophilicity of the compound and its relative retention time in the RP-HPLC run (as gleaned through database information and preliminary calibration with commercially-available ultra-pure standards, as previously described). Relative quantitative variations of intact mass peak areas for each metabolite assigned through MS were normalized against controls (0 μM $CdCl_2$) and plotted with GraphPad Prism 5.0 (GraphPad Software Inc. La Jolla, CA,USA).

2. Results and Discussions

From physiology to proteomics and metabolomics

Recent physiological evidence in the literature[12] indicated that *Cakile maritima Scop. Sea Rocket* (European Sea Rocket) could accumulate twice as much Cd in the shoots in comparison to *Brassica juncea Czern*, while remaining apparently unaffected in terms of photosystem activity, transpiration rate, water use efficiency and stomatal conductance. Conversely, minor growth retardation was still achieved' under acute Cd stress (100 μM)[12]. This is suggestive of the fact that tolerance and accumulation of Cd in this species might result in physiological homeostasis, which is governed by proteomics and metabolic adaptations that are elusive to detect when merely focusing on the main physiologically relevant criteria. In the light of the recent strides in the field of proteomics[23] and metabolomics[24] application to environmental issues and, in particular, to plant responses to heavy metal stress, we hereby decided to perform an integrated proteomics and metabolomics analysis to gain further insights into the molecular responses to Cd stress in *Cakile maritima Scop. Sea Rocket*.

Proteomics

Adaptations to Cd stress are known to be driven by altered gene expression[6,25], or are rather accompanied by alterations to the proteome[5] and integrity of multi-protein complexes[10,12]. Protein changes have been indeed investigated in *Cakile maritima Scop. Sea Rocket* in response to salt stress[16], which helped highlight abiotic stress-dependent adaptations in this species.

Therefore, in the present study we preformed 2DE gel-based analyses to assay the responses of the *Cakile maritima Scop. Sea Rocket* leaf proteome to Cd toxicity. Results are summarized in electronic supplementary information **(ESI)**, whereby spot numbers and their quantitative trends (fold-change variations) are reported by indicating the up and down-regulation of a specific spot when comparing untreated controls to either leaves from plants exposed to 25 or 100 μM $CdCl_2$, or when comparing differential expression patterns in response to mild (25 μM) or heavy (100 μM) Cd stress. Results are reported indicating the spot number, the relative NCBI gene identifier, the theoretical molecular weights and p*I*, Mascot scores and the number of peptides identified via nanoHPLC-MS/MS, along with fold change variations as gleaned via quantitative analysis through the software PDQuest. Exposure to 25 or 100 μM $CdCl_2$ resulted in the statistically significant (p-value < 0.05 ANOVA, fold-change > $\left|1.5\right|$) variation in abundance of a total of 36 unique protein spots across groups (either control vs 25 μM $CdCl_2$ – **Figure 1.A**; control vs 100 μM $CdCl_2$ – **Figure 1.B**; or 25 μM $CdCl_2$ vs 100 μM $CdCl_2$ – **Figure 1.C**).

Differential proteomics revealed that exposure to mild (25 μM) and high (100 μM) Cd stress promoted the upregulation of the glutathione-ascorbate system.

Down-regulation of photosynthetic machinery by Cd stress is a known phenomenon.[26]. Exposure to mild Cd stress (25μM) did not promote a massive down-regulation of proteins involved in light harvesting complex II and photosystem II activity as it has been recently observed in *Brassica juncea Czern*[5,27], while it resulted in the downregulation of photosystem II oxygen-evolving complex protein 2 (PSbP - spots no. 3101 and 5204 – (ESI), Figure 1.A). This is relevant in that it justifies the physiological results from Taamalli and colleagues[12] about the lack of perturbations in photosystem efficiency, while it supports the observed down-regulation of non photochemical quenching NPQ reactions[12]. Indeed, PSbPs has been recently suggested to modulate heat dissipating reaction that contained radicals species via non photochemical quenching (NPQ)[28]. Proteomics technologies have been previously used to document alterations to PSbP in response to heavy metal stress[31], though increases in the levels of PSbPs had

been previously reported in relation of soybeans responses to mild Cd stress[29]. On the other hand, increased levels of the RubisCO large subunit (spot 1601 – electronic supplementary information **(ESI)** in response to heavy metal stress are consistent with the literature in other hyperaccumulator species[26].

Exposure to heavy metals, in particular Cd, triggers the generation of ROS, which results in cell depletion of the major thiol containing antioxidant compounds and enzymes, thus disrupting the plant redox homeostasis[6,26,27]. The results are dramatic in that ROS promote the accumulation of peroxidized lipids and fragmentation of proteins[5], together with the disassembly of multi-protein complexes[10,19]. To counter oxidative stress, plants have evolved robust antioxidant defense mechanism which include both enzymatic and non-enzymatic components[30]. Since halophytes are correlated with a more efficient antioxidant system[31], they might also be more efficient in coping with heavy metals stress than common plants. An example is represented by the common ice plant (*Mesembryanthemum crystallinum*), a facultative halophyte that responds to Cd stress through the activation of the peroxidase system[32]. In *Cakile maritima Scop. Sea Rocket*, it has been recently evidenced that salt stress corresponded to a significant accumulation of stress-response (catalase and oxalic acid oxidase) enzymes and potent leaf antioxidant activity (both enzymatic and non-enzymatic) [16]. When challenging mild and heavy Cd stress, *Cakile maritima Scop. Sea Rocket* resulted in the promotion of anti-oxidant responses by up-regulating glutathione homeostasis (plastidic glutamine synthetase – spots no. 1601 and 5505; glutathione S-transferase – spot no. 7206 – electronic supplementary information **(ESI), Figure 1.A**) and the glutathione-ascorbate metabolism (dehydroascorbate reductase - spot no. 7206 – electronic supplementary information **(ESI), Figure 1.A** and **B**). Further exacerbation of Cd-induced oxidative stress at elevated Cd concentrations (100 μM) promoted anti-oxidant defenses through the up-regulation of SOD1 (spot no. 7107 – electronic supplementary information **(ESI), Figure 1.B**). This is consistent with the literature, since most of the proteomic papers in the field have so far documented a positive correlation between tolerance and increased abundance of scavenger proteins[26], including SOD are most important [19,26,33]. SOD plays a pivotal role in cellular defense against oxidative stress, as its activity directly modulates the amount of $O^{\cdot}2$ and H_2O_2, the two important substrates for Haber–Weiss reactions[34]. The excess $O^{\cdot}2$ radical generated under heavy metal-stress usually disproportionate into H_2O_2 by the action of SOD, which is in turn metabolized by the components of the ascorbate–GSH cycle.

Mild Cd stress promoted energy metabolism at the triose-phosphate and ATP-generation level and CO_2 homeostasis

As it has been recently reviewed[26], in order to maintain the normal growth and development under stressed environment, plants need to up regulate metabolic pathways such as glycolysis and tricarboxylic acid (TCA) cycle. Faster catabolism is also useful to produce more reducing power to compensate high-energy demand in the heavy metal exposed cell[29]. Concordantly, we hereby observed the up-regulation of the glycolytic enzyme phosphoglycerate kinase (spot no. 5505) and mitochondrial F1 ATP synthase beta subunit (spot no. 6603 – which was found to be fragmented in response to Cd stress in *Brassica juncea Czern*[5] (electronic supplementary information **(ESI)**).

Up-regulation of carbonic anhydrase (spot no. 7206 – electronic supplementary information **(ESI)**, **Figure 1.A** and **B**) in response to Cd stress might represent another species-specific adaptation, if we consider that the very same protein was found to be down-regulated in *Brassica juncea Czern* under the same experimental conditions[5]. Carbonic anhydrase is a zinc (divalent ion) metalloenzyme catalysing the reversible hydration of CO_2 to produce H^+ and HCO_{3-}. However, it also participates in the stimulation via carbamylation of RubisCO at low Cd concentrations[35].

Vacuolar transporters for heavy metal detoxification were up-regulated by Cd stress

The final step of heavy metal detoxification involves sequestering of either free or phytochelatin bound-heavy metal complexes into cell vacuoles[36]. This accumulation is mediated by tonoplast-bound cation/proton exchanger, P-type

ATPase and ATP-dependent ABC transporter[36]. As the vacuoles or apoplasts have limited metabolic activity, accumulations of heavy metals in these compartments reduce the toxic effects of heavy metals. Notably, in the present study we observed a statistically significant up-regulation of vacuolar transporters (nucleotide-binding subunit of vacuolar ATPase – spots no. 3601 and 3602 – electronic supplementary information **(ESI), Figure 1.A and B**) both in leaves from plants exposed to mild and heavy Cd doses. These results are consistent with iTRAQ analysis of Cd-exposed barley leaf mesophyll tonoplast[37], and other proteomics analyses on rice roots and leaves exposed to Cd[38,39].

Exposure to high (100 µM) Cd stress partly affected photosystem integrity and metabolic activity, through the up-regulation of enzymes from the Calvin cycle and glutathione-ascorbate homeostasis

Plant exposure to high doses of $CdCl_2$ resulted in further alterations at the transcriptional (chloroplast elongation factor Tub - spot no. 2502) and translational (RNA binding proten cp31 - spot no. 0303) level (electronic supplementary information **(ESI), Figure 1.B**.

Interestingly, while the deregulation of photosystem II subunit O-2 (spot no. 3303) and photosystem I light-harvesting chlorophyll a/b-binding protein (spot no. 6102) suggest that elevated Cd concentration start showing deleterious effects on photosystem integrity (in analogy to other hyperaccumulator plants[5]), on the other hand the observed up-regulation of the photosystem II stability/assembly factor (spot no. 2502 – electronic supplementary information **(ESI), Figure 1.B**) indicate a peculiar mechanism that might underpin the recently documented[12] improved capacity *Cakile maritima Scop. Sea Rocket* to cope with Cd-induced stress while maintaining the homeostasis at the photosystem level. Indeed, this protein is essential for photosystem II (PSII) biogenesis, since it is required for assembly of an early intermediate in PSII assembly that includes D2 (psbD) and cytochrome b559[40]. Analogously, the up-regulation of Peptidyl-prolyl cis-trans isomerase CYP38, chloroplastic (spot no. 1502 – electronic supplementary information **(ESI), Figure 1.**B) plays a protective role in the stability and biogenesis of PSII. In fact PPIAse family catalyzes the cis-trans isomerization of proline imidic peptide bonds in oligopeptides and is required for the assembly and stabilization of PSII[41] . It's also observed the accumulation of germin-like protein (spot no. 7102 - electronic supplementary information **(ESI), Figure 1.B**), a protein of the germin family that plays a role in mediating plant responses to biotic and abiotic stresses (especially salt and heavy metal stress)[42] .

However, at 100 µM dose proteomics adaptation start involving cell metabolism, in that plant responses to heavy Cd stress included the deregulation of energy metabolism at the triose phosphate level (decrease in pyruvate dehydrogenase - spot no. 4503; and ATP synthase CF1 beta subunit – spot no. 6604) and up-regulation of rate limiting enzymes that mediate the branching from glycolysis to the pentose phosphate pathway (PPP) and the Calvin cycle (sedoheptulose bisphosphatase – spot no. 2502; RubisCO – spots no. 2102, 2602, 7106; and fructose bisphophatase – spot no. 2502 – electronic supplementary information **(ESI), Figure 1.B**). This metabolic behavior would serve the purpose to balance carbon assimilation via the light-independent reactions in the Calvin cycle or rather promote the reduction of $NADP^+$ to NADPH via the PPP, as to replenish the reservoirs of the reducing coenzyme that plays an essential role in the maintenance of GSH homeostasis. A tentative clue to this question will stem from the metabolomics analyses performed in the present study, as discussed below.

In comparison to mild Cd stress, high Cd stress further down regulated carbon dioxide homeostasis, but up-regulated of Calvin cycle enzymes and PAP3 to stabilize thylakoid membrane structures in response to Cd stress

When comparing 2DE gels from leaves exposed to 100µM against 25µM $CdCl_2$, consistently with what anticipated above, it emerged that heavy metal stress promoted the down-regulation of energy metabolism by deregulating both

mitochondrial and chloroplast ATP synthases (spots no. 5605 6603), while promoting the up-regulation of Calvin cycle enzymes sedoheptulose bisphosphatase and RubisCO. Cd stress at heavy doses also resulted in the significant deregulation of the chloroplast carbonic anhydrase protein (spot no. 7205), consistently with the observation in *Brassica juncea Czern*[5] and *Picris divaricata*[43]. However, when considering the relative fold-change variation of the spot 7206 (carbonic anhydrase) in 25 and 100 μM leaves in comparison to untreated controls (+2.63 and +3.43, respectively), and comparing the localization of the two spots (7205 and 7206) on 2DE maps (**Figure 1.B and C**), it is immediately evident that these spots are likely to represent two differentially post-translationally modified isoforms of carbonic anhydrase (maybe phosphorylated), since the spots share the same apparent MW albeit different pIs[45] , rather than an actual de-regulated expression of the protein *per se*. Further investigations are awaited in the future.

Increased levels of plastid lipid associated protein PAP3 (spots no. 0501) are consistent with previous reports in the literature indicating that PAPs accumulate in in leaf chloroplasts under abiotic stress conditions, whereby they are used to store hydrophobic compounds or stabilize the structure of thylakoid membranes upon environmental constraints[45] .

Metabolomics

In analogy with our previous report on *Brassica juncea Czern* responses to Cd stress[5], metabolomics analyses were performed to integrate and expand the physiological and protoemics observations. Results have been graphed in a pathway-wise fashion, in the following order: phytochelatins (**Figure 2**) and glutathione homeostasis (**Figure 3**), the pentose phosphate pathway (PPP – **Figure 4**), glycolysis (**Figure 5**), the Krebs cycle (**Figure 6**) and other metabolic pathways (including hormone responses – **Figure 7**).

Oxidative stress: alterations to glutathione homeostasis, phytochelatins, sulphur metabolism .

As anticipated above, Cd stress is accompanied by increased oxidative stress, which is counterattacked through the synthesis of thiol-containing compounds that either detoxify ROS or chelate the toxic heavy metal, as to minimize the binding of divalent Cd ions to functionally important proteins[46] . Thiol group containing chelators thus participate in Cd sequestration from the cytosol and its transport to the vacuoles. The phytochelatins (PCs) and metallothioneins (MTs), the two best characterized cysteine-rich heavy metal (HM) binding peptides/proteins, play crucial roles in HM tolerance mechanism by chelating cations[47]. Accumulation of PCs in response to heavy metal (and Cd) stress is a common feature in plant hyperaccumulators (reviewed in Hossain and Komatsu[27]) and *Cakile maritima Scop. Sea Rocket* makes no exception (**Figure 2**). In particular, we detect a statistically-significant accumulation of PC2 and PC3 ($p<0.01$ and 0.05, respectively) especially in response to high doses of Cd (100μM), whereby we could also detect a significant accumulation of Cd-chelating PCs (**Figure 2**).

Since PCs are synthesized from glutathione (GSH) by the enzyme PC synthase[48], modulation of proteins and amino acids (anabolic substrates) involved in PC biosynthesis have been the most widely studied in response to Cd. In **Figure 3** we document how oxidative stress in response to Cd resulted in the Cd concentration dependent decline in the level of GSH (**Figure 3.**A) and in the progressive accumulation of the oxidized form of glutathione (GSSG – **Figure 3.B**). On the other hand, aminoacid precursors to GSH and PCs tended to accumulate in a Cd-dependent fashion (including glutamic acid and cysteine – **Figure 3.C** and **D**, respectively – two rate-limiting aminoacid substrates for the biosynthesis of the tripeptide GSH[49].

As indicated above, responses to Cd stress in *Cakile maritima Scop. Sea Rocket* also included the up-regulation of glutathione homeostasis, which involved the biosynthesis of the glutamate precursor, glutamine, via the plastidic glutamine synthetase (spots no. 1601 and 5505) and glutathione S-transferase (spot no. 7206 – electronic supplementary information **(ESI), Figure 1.A**), the latter enzyme being involved in the conjugation of thiol-containing GSH

derivatives to xenobiotic compounds for detoxification purposes. In line with the proteomics results, glutamine was found to accumulate in a statistically-significant fashion (*p-value* < 0.05 ANOVA) in response both to mild and higher Cd concentration.

As it has been recently reviewed[50], anti-oxidant defenses in response to oxidative stress further include the ascorbate-glutathione cycle, also known as the Foyer-Halliwell-Asada cycle, whereby superoxide can be converted to H_2O_2 by SOD, hereby up-regulated in response to high doses of $CdCl_2$, (spot no. 7107 – electronic supplementary information **(ESI), Figure 1.B**). Then, H_2O_2 is further detoxified by ascorbate peroxidase, whereby monodehydroascorbate is produced, which can spontaneously dismutate to ascorbate and dehydroascorbate, which is recycled to ascorbate by the GSH-dependent enzyme dehydroascorbate reductase (up-regualted in response to Cd stress in the present study - spot no. 7206 – electronic supplementary information **(ESI), Figure 1.A** and **B**). Consistently with proteomics results, metabolomics analyses highlighted a Cd-dependent increase in the levels of ascorbate (**Figure 3.F**).

Proteomics responses to drought stress in *Cakile maritima Scop. Sea Rocket* have been recently related to the accumulation of glutamine synthase, but also to the up-regulation of one-carbon metabolism through the salt stress-dependent increase in the levels of serine hydroxymethyl transferase[16] . Indeed, during the last few years, it has rapidly emerged the relevance of the cross-talk between GSH homeostasis and one-carbon metabolism, that provides serine-derived glycine and cysteine substrates for the biosynthesis of the tripeptide glutathione, the latter through a reaction involving serine and homocysteine intermediates and the production of cystathionine[51] . In the absence of results indicating actual metabolic fluxes via stable isotope labeling, the hereby observed accumulation of homocysteine (**Figure 3.G**) and deregulation of cystathionine (**Figure 3.H**) might give rise to two opposite interpretations, either suggesting the depression or more rapid fluxing (thus lower accumulation of the intermediate cystathionine) of cysteine biosynthesis. On the other hand, no significant changes were observed in the levels of serine in response to Cd-induced stress (data not shown).

PPP and the Calvin cycle were affected by Cd stress, which utterly promoted the accumulation of triose-phosphate and the glyoxylate precursor phosphoglycolate to promote photorespiration

The maintenance of the redox homeostasis is basically dependent on the GSH/GSSG and ascorbate/dehydroascorbate ratios, both being (directly or indirectly) dependent on NADPH-involving reactions to restore the reduced form of the redox couple. The main NADPH generating pathway in eukaryotes is represented by the oxidative phase of the pentose phosphate pathway (PPP), a key metabolic pathway branching from glycolysis at the glucose 6-phosphate level. A rate limiting step upstream to the PPP is represented by the breakdown of fructose bisphosphate (hereby decreasing in response to high doses of Cd – **Figure 4.A**) by fructose bisphosphatases (up-regulated in response to Cd stress - spot no. 2502 – electronic supplementary information **(ESI), Figure 1.B**). Over-activation of the oxidative phase of the PPP would result in the accumulation of pentose phosphate sugars (such as ribose phosphate - **Figure 4.B**). On the other hand, no significant alteration was observed in the levels of non-oxidative phase PPP intermediates sedoheptulose phosphate and erythrose phosphate (**Figure 4.C** and **D**, respectively), the latter apparently following a trend towards decrease in a Cd-dependent fashion. In plants, light dependent reactions provide NADPH and ATP to fuel carbon fixation through light independent reactions in the Calvin cycle. In this view, it is worthwhile to stress that no significant alteration was observed in the levels of $NADP^+$ and NADPH (**Figure 4.E** and **F**), the latter being partly consumed (albeit not in a statistically significant fashion) only at high doses of Cd.

It is known[30] that plants attempt to cope with heavy metal stress by up-regulating Calvin cycle enzymes, such as RubisCO (confirmed here in spots no. 2102, 2602, 7106; electronic supplementary information **(ESI), Figure 1B**),

which in turn promotes the accumulation of Calvin cycle precursor and intermediate metabolites. In this view, it is worth noting that the Calvin cycle rate-limiting precursor ribulose 1,5 bisphosphate was significantly accumulated in leaves from plants exposed to high doses of Cd (**Figure 4.G**).

At the same time, proteomics results highlighted the high Cd dose-dependent up-regulation of sedoheptulose bisphosphatase (spot no. 2502 - electronic supplementary information **(ESI), Figure 1.B**). Metabolomics results are consistent with these observations, in that we could detect significantly ($p<0.05$ ANOVA) lower levels of sedoheptulose biphosphate (**Figure 4.H**) in leaves from plants exposed to 100μM $CdCl_2$.

However, it is also relevant to note that RubisCO is a bifunctional enzyme, with the capacity to competitively use CO_2 or O_2. Of note, plants exposed to stress exhibit enhanced photorespiration[5,52], that is believed to be a wastefull process involved in loss of carbon as CO_2. The ultimate goal of the Calvin cycle is the production of soluble sugars through the build-up of the triose phosphate compound glyceraldehyde 3-phosphate via the intermediates 3-phosphoglycerate and bisphosphoglycerate. On the other hand, photorespiration yields the accumulation of phosphoglycerate and phosphoglycolate, a metabolic intermediate that is further shuttled from the chloroplast to the peroxisome to give rise to glyoxylate and the toxic hydrogen peroxide. However, glyoxylate is transaminated to glycine, and then, after its conversion to serine in the mitochondria, it is recycled into hydroxypyruvate and glycerate to fuel back the Calvin cycle. Increased photorespiration is an emerging adaptive response to abiotic stresses[53,54], which could fuel the glyoxylate cycle in *Cakile maritima Scop. Sea Rocket* in response to drought stress through the up-regulation of the glyoxylate cycle enzyme malate synthase[19]. Although in the present study we could not find any direct evidence of the increase in the glyoxylate cycle, increased rates in RubisCO-mediated photorespiration are hinted by the statistically significant accumulation of the byproduct phosphoglycolate (**Figure 4.I**) in a dose-dependent fashion in response to mild and heavy Cd stress ($p<0.05$ *and* 0.001, respectively). However, while we had previously reported phenomenon for *Brassica juncea Czern* in response to Cd stress, in that species the observed decrease in transpiration and stomatal conductance resulted in the accumulation of intercellular CO_2 [5]. On the other hand, in *Cakile maritima Scop. Sea Rocket* this did not happen, since no significant alteration of CO_2 physiology have been observed in response to Cd stress[12].

Accumulated glyceraldehyde 3-phosphate may serve as a substrate to promote the synthesis of triglycerides, while it is accompanied by erucic acid accumulation

In the previous paragraphs we have anticipated that Cd stress is often associate with the up-regulation of energy metabolism-related enzymes, including glycolysis and the TCA. This is due to the necessity to maintain energy homeostasis to sustain carbon fixation and (indirectly) redox reactions[30]. In the present study, plant exposure to Cd resulted in the accumulation of early glycolytic precursors (either hexose and triose phosphates – **Figure 5.A** and **B**, respectively). This might be due to a blockade of glycolysis at the early steps to promote a metabolic shift to the PPP, as to respond to higher demands for NADPH generation (as explained above). On the other hand, this might also result from an exacerbation of carbon fixation reactions utterly yielding glyceraldehyde 3-phosphate and hexose sugars, the conversion of 3-phosphoglycerate to bisphosphoglycerate being catalyzed by the enzyme phosphoglycerate kinase (hereby increased in response to Cd stress – spot no. 5505 – electronic supplementary information **(ESI)**).

Accumulation of glyceraldehyde 3-phosphate might also serve the purpose to build up glycerol backbones to sustain the biosynthesis of triacylglycerols (TAG), which make up most of lipids in *Cakile maritima Scop. Sea Rocket* seed oil. *C. maritime*, in fact, is characterized by high seed oil content (up to 39% on dry weight basis), with triacylglycerols (TAG) representing the 97% of the total fatty acids (mostly erucic acid, of economic interest in that it is used in plastic and painting industries)[55–57]. *Cakile maritima Scop. Sea Rocket* can either behave as a salt-sensitive or relatively salt-tolerant

species at the early developmental stages, while it is either salt-requiring or facultative halophyte, respectively, at the vegetative and reproductive stages[58,59]. In this view, it is relevant to note that the detected levels of erucic acid (the most abundant fatty acid in *Cakile maritima Scop. Sea Rocket* seed oil TAG) were significantly (*p-value* < 0.05 ANOVA) higher in heavily Cd-stressed plants (see below) , further stressing the biological relevance of metabolic adaptations to abiotic stresses in this plant.

Consistently, triose metabolites downstream to phosphoglycerate in glycolysis tended to decrease, especially in response to higher doses of Cd (**Figure 5.C** and **D**). On the other hand, anaerobic termination of glycolysis via lactic fermentation (**Figure 5 E**) was not apparently altered by Cd exposure, as pyruvate is preferentially shuttled to the mitochondria in the form of acetyl-CoA to sustain the TCA cycle. However, proteomics results suggest that another adaptive response to Cd stress might lie at this step, since the exposure to higher doses of Cd resulted in the de-regulated expression of the enzyme responsible for the conversion of pyruvate to acetyl-CoA, pyruvate dehydrogenase (spot no. 4503). To further delve into this issue, we thus focused on mitochondrial metabolism.

Cd depressed the TCA cycle downstream to citrate, probably fueling glutamate synthesis to promote anabolism of glutathione

ATP synthesis in plants mostly relies on light dependent reactions in chloroplast and ATP synthases, which depend upon the proton gradient fueled by the oxidative phosphorylation in mitochondria. Down regulation of ATP synthesis was observed only in response to high doses of Cd (**Figure 5.F**), which are both suggestive of down regulation of photosystem efficiency or altered mitochondrial metabolism. Since physiological and proteomics analyses did not reveal any significant alteration of the former, mitochondrial metabolism appeared to be the most likely candidate. In line with this, it is worthwhile recalling that proteomics results evidenced a Cd dose-dependent deregulation of mitochondrial ATP synthases (spot no. 6603 - electronic supplementary information **(ESI), Figure 1.C**). Of note, opposite trends were observed for salt challenged leaves of *Cakile maritima Scop. Sea Rocket*[22], which might underlie specific adaptations to different abiotic stresses in this plant.

In terms of mitochondrial metabolism, previous studies had suggested that accumulation of negatively charged organic acid intermediates of the TCA (especially α-ketoglutarate, fumarate and malate) might promote beneficial effects in response to heavy metal stress, as they might directly contribute Cd chelation and long distance transport to the aerial parts[55] . However, we could not confirm such metabolic adaptation in *Brassica juncea Czern*[5] nor in the present study, whereby the levels of Krebs cycle intermediates downstream to citrate were decreased in a Cd dose-dependent fashion (**Figure 6.A, C-F**). Conversely, citrate levels were increased in response to mild Cd stress (**Figure 6.B**), which is suggestive of a likely metabolic blockade downstream to it in the TCA cycle. One tentative hypothesis is that citrate might fuel the biosynthesis of glutamate through the transamination of the α-ketoglutarate TCA intermediate (downstream to citrate and upstream to succinyl CoA), thus providing a key building block to further sustain the biosynthesis of GSH and its derivatives (i.e. PCs). Although further studies with stable metabolic tracers are mandatory, it is interesting to note that a similar behavior has been already documented for tobacco plants exposed to Cd stress[44] .

Osmoprotectants betaine and proline, methyl jasmonate and salicylic acid responded to heavy Cd stress and deserve further investigations in the future

Halophytes can withstand the ionic and the osmotic components of salt stress owing to their ability to synthesize osmoprotectants in order to maintain a favorable water potential gradient and to protect cellular structures[60] . Betaine

(also known as trimethylglycine or glycynebetaine) and proline[61], in particular, have significant beneficial functions under metal stress by three major actions, namely metal binding, antioxidant defense, and signaling[11,62] .

Up-regulation of proline and betaine metabolism in *Cakile maritima Scop. Sea Rocket* in response to salt stress has been recently documented through proteomics analyses[16] . In the present study, betaine and proline levels increased significantly in response to Cd stress, in a dose-dependent fashion[63] (**Figure 7.B** and **C**, respectively).

Similarly, polyamines may be involved in the protection of cellular structures under drought and salt stress conditions[64,65], but their specific role in plants under metal stress is only poorly documented[11]. A common interpretation is that since heavy metal stress induces both a secondary water stress[66] and oxidative damages to cellular structures[31] , the ability of halophytes to synthesize those osmoprotectants may be involved in their ability to cope with heavy metals[11,60]. Unfortunately, the metabolomics workflow exploited in the present study did not allow to detect polyamines. However, it is worth considering the metabolism of S-adenosylmethionine (SAM). SAM is a primary donor of methyl groups, which further yields S-adenosyl-L-homocysteine (SAH) that is metabolised to eventually regenerate methionine. SAM participates in the biosynthesis of the polyamines spermidine and spermine from putresceine via the enzymes spermine and spermidine synthases. In addition, SAM is involved in the biosynthesis of choline, a precursor to betaine, other than of methyljasmonate[67], which we recently found to be up-regulated in response to Cd stress in *Brassica juncea Czern*[5]. Of note, in *Cakile maritima Scop. Sea Rocket,* salt stress responses also included the up-regulation of the enzyme S-adenosylmethione synthetase[19] . In the present study, no Cd-dependent alterations were observed in terms of SAM and SAH (data not shown), which are also involved in the reconversion of methionine to cysteine (we have detailed in the previous paragraphs the central role of cysteine and thiol metabolism in response to Cd stress in *Cakile maritima Scop. Sea Rocket*). On the other hand, methyljasmonate increase in response to high Cd stress was extremely significant (*p-value* < 0.001 – **Figure 7.D**). While in *Brassica juncea Czern* Cd stress promoted a dose-dependent increase in absisic acid and decrease in salicylic acid[5], metabolomics results showed an opposite behavior in *Cakile maritima Scop. Sea Rocket* (**Figure 7.E** and **F**). This is relevant in that salicylic acid seems to contribute to adaptive responses to Cd stress in rice[68] .

4. Conclusion

Cakile maritima Scop. Sea Rocket is known to behave like a promising bioaccumulator and phytoextractor for phytoremediation purposes, since Cd accumulation in roots and translocation to the aerial parts was proportionally to Cd concentration[12] . This plant seemed to be naturally equipped to withstand even high doses of Cd pollution, while showing only minor growth retardation at the highest doses[12] . From a physiological standpoint, prolonged exposure to Cd resulted in minor effects on transpiration, stomatal conductance and net CO_2 assimilation, while Cd stress did not affect pigment composition, resulting only in minor deregulation of chlorophyll b and no significant variation in terms of photosystem II efficiency[12], conversely to what previously reported for other more extensively investigated model species of the *Brassicaceae* family[5,12] **(Figure 8).** Exposure to mild (25 μM) and heavy (100 μM) Cd stress promoted anti-oxidant defenses through the upregulation of the phytochelatin anabolism, glutathione-ascorbate system (confirmed both at the protein and metabolic level), while de-regulating flow rate of electrons from the reaction centers in like fashion to responses to salt stress. Such metabolic adaptations involved a boost in sulphur metabolism and, apparently, a cross-talks with one-carbon metabolism (providing cysteine and glycine building blocks for the tripeptide GSH, as a shared common feature with *Cakile maritima Scop. Sea Rocket* responses to salt stress[16] . Metabolic adaptation also involved the up-regulation of the PPP and Calvin cycle (both at the enzyme and metabolite level), which utterly promoted the maintenance of $NADPH/NADP^+$ homeostasis, other than the accumulation of triose-phosphates (serving as anabolic intermediates for triacylglycerol biosynthesis) and the glyoxylate precursor phosphoglycolate, to promote photorespiration. However, homeostasis in carbon dioxide metabolism was preserved by the up-regulation of carbonic anhydrase, consistently with previously observed unaltered stomatal conductance and transpiration in leaves from *Cakile maritima Scop. Sea Rocket* exposed to Cd[12] , while in *Brassica juncea Czern* the observed decrease in transpiration and stomatal conductance resulted in the accumulation of intercellular CO_2 [5]. On the other hand, Cd depressed ATP synthesis in the mitochondria (through a dose-dependent deregulation of mitochondrial ATP synthases), and the TCA cycle downstream to citrate, probably fueling glutamate synthesis to promote anabolism of glutathione. Overall, *Cakile maritima Scop. Sea Rocket* appeared to be naturally equipped to cope with osmotic stress, as it clearly emerged from the observed Cd-dependent increase in the levels of PCs and other osmoprotectants (such as betaine and proline) and, at the protein level, by the up-regulation of proteins involved in thiol compound-dependent sequestration of xenobiotic toxic compounds and translocation into the vacuoles (such as glutathione S-transferase or vacuolar transporters). Finally, the observed Cd-dependent increase in the levels of methyl jasmonate and salicylic acid will deserve further investigations in the future.

Acknowledgments

The authors are grateful to Dr. Ghnaya T and Dr Abdelly C for their support. LZ and ADA are supported by mobility studentship funds and post-doctoral research grant by the Interuniversity Consortium for Biotechnologies (CIB).

References

1. L. Järup, Br. Med. Bull., 2003, 68, 167–182.
2. L. Järup and A. Åkesson, Toxicol. Appl. Pharmacol., 2009, 238, 201–208.
3. A. D'Alessandro and L. Zolla, J. Proteome Res., 2012, 11, 26–36.
4. G. Visioli and N. Marmiroli, J. Proteomics, 2013, 79, 133–145.
5. A. D'Alessandro, M. Taamalli, F. Gevi, A. M. Timperio, L. Zolla, and T. Ghnaya, J. Proteome Res., 2013, 12, 4979–4997.
6. G. DalCorso, S. Farinati, and A. Furini, Plant Signal. Behav., 2010, 5, 663–667.
7. S. M. Gallego, L. B. Pena, R. A. Barcia, C. E. Azpilicueta, M. F. Iannone, E. P. Rosales, M. S. Zawoznik, M. D. Groppa, and M. P. Benavides, Environ. Exp. Bot., 2012, 83, 33–46.
8. L. Sanità di Toppi and R. Gabbrielli, Environ. Exp. Bot., 1999, 41, 105–130.
9. M. P. Benavides, S. M. Gallego, and M. L. Tomaro, Braz. J. Plant Physiol., 2005, 17, 21–34.
10. M. I. Qureshi, G. M. D'Amici, M. Fagioni, S. Rinalducci, and L. Zolla, J. Plant Physiol., 2010, 167, 761–770.
11. E. Manousaki and N. Kalogerakis, Int. J. Phytoremediation, 2011, 13, 959–969.
12. M. Taamalli, R. Ghabriche, T. Amari, M. Mnasri, L. Zolla, S. Lutts, C. Abdely, and T. Ghnaya, Ecol. Eng., 2014, 71, 623–627.
13. J. Rozema and T. Flowers, Science, 2008, 322, 1478–1480.
14. I. H. Wahla and M. B. Kirkham, Environ. Pollut. Barking Essex 1987, 2008, 155, 271–283.
15. H. Zhang, B. Han, T. Wang, S. Chen, H. Li, Y. Zhang, and S. Dai, J. Proteome Res., 2012, 11, 49–67.
16. A. Debez, H.-P. Braun, A. Pich, W. Taamalli, H.-W. Koyro, C. Abdelly, and B. Huchzermeyer, J. Proteomics, 2012, 75, 5667–5694.
17. A. Debez, D. Saadaoui, B. Ramani, Z. Ouerghi, H.-W. Koyro, B. Huchzermeyer, and C. Abdelly, Environ. Exp. Bot., 2006, 57, 285–295.
18. M. Fagioni, G. M. D'Amici, A. M. Timperio, and L. Zolla, J. Proteome Res., 2009, 8, 310–326.
19. A. Shevchenko, M. Wilm, O. Vorm, and M. Mann, Anal. Chem., 1996, 68, 850–858.
20. A. D'Alessandro, F. Gevi, and L. Zolla, Mol. Biosyst., 2011, 7, 1024–1032.
21. E. Melamud, L. Vastag, and J. D. Rabinowitz, Anal. Chem., 2010, 82, 9818–9826.
22. M. Kanehisa and S. Goto, Nucleic Acids Res., 2000, 28, 27–30.
23. P. Muller, X. Li, and K. K. Niyogi, Plant Physiol., 2001, 125, 1558–1566.
24. J. L. Luque-Garcia, P. Cabezas-Sanchez, and C. Camara, TrAC Trends Anal. Chem., 2011, 30, 703–716.
25. F. Villiers, C. Ducruix, V. Hugouvieux, N. Jarno, E. Ezan, J. Garin, C. Junot, and J. Bourguignon, Proteomics, 2011, 11, 1650–1663.
26. N. Fusco, L. Micheletto, G. D. Corso, L. Borgato, and A. Furini, J. Exp. Bot., 2005, 56, 3017–3027.
27. Z. Hossain and S. Komatsu, Front. Plant Sci., 2012, 3, 310.
28. S. Alvarez, B. M. Berla, J. Sheffield, R. E. Cahoon, J. M. Jez, and L. M. Hicks, Proteomics, 2009, 9, 2419–2431.
29. K. K. Niyogi, X.-P. Li, V. Rosenberg, and H.-S. Jung, gll., 2005, 56, 375–382.
30. M. A. Hossain, P. Piyatida, J. A. T. da Silva, and M. Fujita, J. Bot., 2012, 2012, e872875.
31. N. Ercal, H. Gurer-Orhan, and N. Aykin-Burns, Curr. Top. Med. Chem., 2001, 1, 529–539.
32. Z. Zhu, G. Wei, J. Li, Q. Qian, and J. Yu, Plant Sci., 2004, 167, 527–533.
33. J. L. Hall, J. Exp. Bot., 2002, 53, 1–11.
34. N. I. Shevyakova, I. A. Netronina, E. E. Aronova, and V. V. Kuznetsov, Russ. J. Plant Physiol., 2003, 50, 678–685.
35. P. Kieffer, J. Dommes, L. Hoffmann, J.-F. Hausman, and J. Renaut, Proteomics, 2008, 8, 2514–2530.
36. A. Siedlecka, P. Gardestrom, G. Samuelsson, L. A. Kleczkowski, and Z. Krupa, Z. NATURFORSCHUNG C, 1999, 54, 759–763.
37. T. Schneider, M. Schellenberg, S. Meyer, F. Keller, P. Gehrig, K. Riedel, Y. Lee, L. Eberl, and E. Martinoia, Proteomics, 2009, 9, 2668–2677.
38. K. Lee, D. W. Bae, S. H. Kim, H. J. Han, X. Liu, H. C. Park, C. O. Lim, S. Y. Lee, and W. S. Chung, J. Plant Physiol., 2010, 167, 161–168.
39. R. Aina, M. Labra, P. Fumagalli, C. Vannini, M. Marsoni, U. Cucchi, M. Bracale, S. Sgorbati, and S. Citterio, Environ. Exp. Bot., 2007, 59, 381–392.
40. J. Meurer, H. Plucken, K. V. Kowallik, and P. Westhoff, EMBO J., 1998, 17, 5286–5297.
41. A. Fu, Z. He, H. S. Cho, A. Lima, B. B. Buchanan, and S. Luan, Proc. Natl. Acad. Sci., 2007, 104, 15947–15952.
42. D. Patnaik and P. Khurana, Indian J. Exp. Biol., 2001, 39, 191–200.
43. R.-R. Ying, R.-L. Qiu, Y.-T. Tang, P.-J. Hu, H. Qiu, H.-R. Chen, T.-H. Shi, and J.-L. Morel, J. Plant Physiol., 2010, 167, 81–87.

44. J. Seo and K.-J. Lee, J. Biochem. Mol. Biol., 2004, 37, 35–44.
45. G. Langenkämper, N. Manac'h, M. Broin, S. Cuiné, N. Becuwe, M. Kuntz, and P. Rey, J. Exp. Bot., 2001, 52, 1545–1554.
46. N. Verbruggen, C. Hermans, and H. Schat, Curr. Opin. Plant Biol., 2009, 12, 364–372.
47. C. Cobbett and P. Goldsbrough, Annu. Rev. Plant Biol., 2002, 53, 159–182.
48. E. Grill, S. Löffler, E. L. Winnacker, and M. H. Zenk, Proc. Natl. Acad. Sci. U. S. A., 1989, 86, 6838–6842.
49. Z. Hossain, M. Hajika, and S. Komatsu, Amino Acids, 2012, 43, 2393–2416.
50. L. Zagorchev, C. E. Seal, I. Kranner, and M. Odjakova, Int. J. Mol. Sci., 2013, 14, 7405–7432.
51. M. C. Reed, R. L. Thomas, J. Pavisic, S. J. James, C. M. Ulrich, and H. F. Nijhout, Theor. Biol. Med. Model., 2008, 5, 8.
52. N.-H. Afef, S. Leila, B. Donia, G. Houda, and C.-H. Chiraz, Am. J. Plant Physiol., 2011, 6, 294–303.
53. S. Kangasjärvi, J. Neukermans, S. Li, E.-M. Aro, and G. Noctor, J. Exp. Bot., 2012, err402.
54. I. Voss, B. Sunil, R. Scheibe, and A. S. Raghavendra, Plant Biol. Stuttg. Ger., 2013, 15, 713–722.
55. T. Ghnaya, H. Zaier, R. Baioui, S. Sghaier, G. Lucchini, G. A. Sacchi, S. Lutts, and C. Abdelly, Chemosphere, 2013, 90, 1449–1454.
56. R. Ksouri, W. M. Ksouri, I. Jallali, A. Debez, C. Magné, I. Hiroko, and C. Abdelly, Crit. Rev. Biotechnol., 2012, 32, 289–326.
57. M. Zarrouk, H. E. Almi, N. B. Youssef, N. Sleimi, A. Smaoui, D. B. Miled, and C. Abdelly, in Cash Crop Halophytes: Recent Studies, eds. H. Lieth and M. Mochtchenko, Springer Netherlands, 2003, pp. 121–124.
58. M. A. Ghars, A. Debez, and C. Abdelly, Commun. Soil Sci. Plant Anal., 2009, 40, 3170–3180.
59. N. B. Amor, A. Jiménez, W. Megdiche, M. Lundqvist, F. Sevilla, and C. Abdelly, Physiol. Plant., 2006, 126, 446–457.
60. I. Lefèvre, G. Marchal, P. Meerts, E. Corréal, and S. Lutts, Environ. Exp. Bot., 2009, 65, 142–152.
61. M. Ashraf and M. R. Foolad, Environ. Exp. Bot., 2007, 59, 206–216.
62. S. S. Sharma and K.-J. Dietz, J. Exp. Bot., 2006, 57, 711–726.
63. A . Bashir , T. Hoffmann , B. Kempf , X. Xie , S.H. Smits , E. Bremer . Microbiology. 2014 160:2283-94
64. A. W. Galston and R. K. Sawhney, Plant Physiol., 1990, 94, 406–410.
65 M. D. Groppa, M. S. Zawoznik, M. L. Tomaro, and M. P. Benavides, Biol. Trace Elem. Res., 2008, 126, 246–256
66. B. Nedjimi and Y. Daoud, Flora - Morphol. Distrib. Funct. Ecol. Plants, 2009, 204, 316–324.
67. P. E. Verslues and S. Sharma, Arab. Book Am. Soc. Plant Biol., 2010, 8, e0140.
68 A . Bashir , T. Hoffmann , B. Kempf , X. Xie , S.H. Smits , E. Bremer . Microbiology. 2014 160:2283-94
69. B. Guo, Y. Liang, and Y. Zhu, J. Plant Physiol., 2009, 166, 20–31.

Figure legends

Figure 1 A representative gel from 2DE analysis of *Cakile maritima Scop. Sea Rocket* leaves exposed to 25 or 100 µM $CdCl_2$, in comparison to untreated controls. Statistically significant differential spots (*p value* < 0.05 and fold change > 1.5) for control vs 25 µM analyses are reported in **A**, while in **B** we indicated those spots showing statistically significant variations in controls in comparison to leaves exposed to 100 µM of $CdCl_2$. In **C**, spots differing between 25 µM and 100 µM gels. Spot protein identifications are reported in electronic supplementary information **(ESI)** . Molecular weight (MW) and p*I* range of the first dimension strips (4-7) are indicated on the appropriate axis.

Figure 2 Variation in the levels of metabolites of the phytochelatins and relative cadmium adducts (A-D) in the leaves of Cakile maritima Scop. Sea Rocket subjected to different Cd concentration, normalized against untreated controls (dashed line at 1 fold change, ± SD calculated across normalized biological replicates of control leaves) . Measurements were performed in triplicate on pooled ground leaves coming from four individual plants per group (control, 25 and 100 µM).
** = p<0.05; ** = p<0.01 *** = p<0.001 ANOVA*

Figure 3 Variation in the levels of metabolites of the glutathione homeostasis (A-D), glutamine/glutamate metabolism (E), glutathione-ascorbate shuttle (F) and cysteine biosynthesis (G-H) in the leaves of *Cakile maritima Scop. Sea Rocket* subjected to different Cd concentration, normalized against untreated controls (dashed line at 1 fold change, ± SD calculated across normalized biological replicates of control leaves). Measurements were performed in triplicate on pooled ground leaves coming from four individual plants per group (control, 25 and 100 µM).
** = p<0.05; ** = p<0.01 *** = p<0.001 ANOVA*

Figure 4 Variation in the levels of metabolic intermediates of the Pentose Phosphate Pathway (PPP) (A,B,C,D,E,F), Calvin cycle (C,D,G,H) and photorespiration (I) in the leaves of *Cakile maritima Scop. Sea Rocket* subjected to different Cd concentration, normalized against untreated controls (dashed line at 1 fold change, ± SD calculated across normalized biological replicates of control leaves) . Measurements were performed in triplicate on pooled ground leaves coming from four individual plants per group (control, 25 and 100 µM).
** = p<0.05; ** = p<0.01 *** = p<0.001 ANOVA*

Figure 5 Variation in the levels of metabolites of glycolytic intermediates (A-E) and adenosine triphosphate (ATP) (F) in the leaves of *Cakile maritima Scop. Sea Rocket* subjected to different Cd concentration, normalized against untreated controls (dashed line at 1 fold change, ± SD calculated across normalized biological replicates of control leaves) . Measurements were performed in triplicate on pooled ground leaves coming from four individual plants per group (control, 25 and 100 µM).
** = p<0.05 ANOVA*

Figure 6 Variation in the levels of metabolites of organic acid of the tricarboxylic acid cycle (A-F) in the leaves of *Cakile maritima Scop. Sea Rocket* subjected to different Cd concentration, normalized against untreated controls (dashed line at 1 fold change, ± SD calculated across normalized biological replicates of control leaves) . Measurements

were performed in triplicate on pooled ground leaves coming from four individual plants per group (control, 25 and 100 μM).

** = p<0.05; ** = p<0.01 *** = p<0.001 ANOVA*

Figure 7 Variation in the levels of erucic acid (A - the main fatty acid component in *Cakile maritima Scop. Sea Rocket* seed oil), the osmoprotectant betaine (B) and proline (C), and the plant hormones, methyl jasmonate (D), abscisic acid (E), and salicylic acid (F) in the leaves of *Cakile maritima Scop. Sea Rocket* subjected to different Cd concentration, normalized against untreated controls (dashed line at 1 fold change, ± SD calculated across normalized biological replicates of control leaves) . Measurements were performed in triplicate on pooled ground leaves coming from four individual plants per group (control, 25 and 100 μM).

** = p<0.05; *** = p<0.001 ANOVA*

Figure 8 An overview of Cadmium stress responses in the halophyte Cakile maritima Scop. Sea Rocket
VHA:is a subunit of V-ATPase DHAR :Dehydro ascorbatereductase GST: Glutathione S-transferase. GERMLP: Germin like protein PAP3 PPIA Prolyl isomerase (also known as peptidylprolyl isomerase

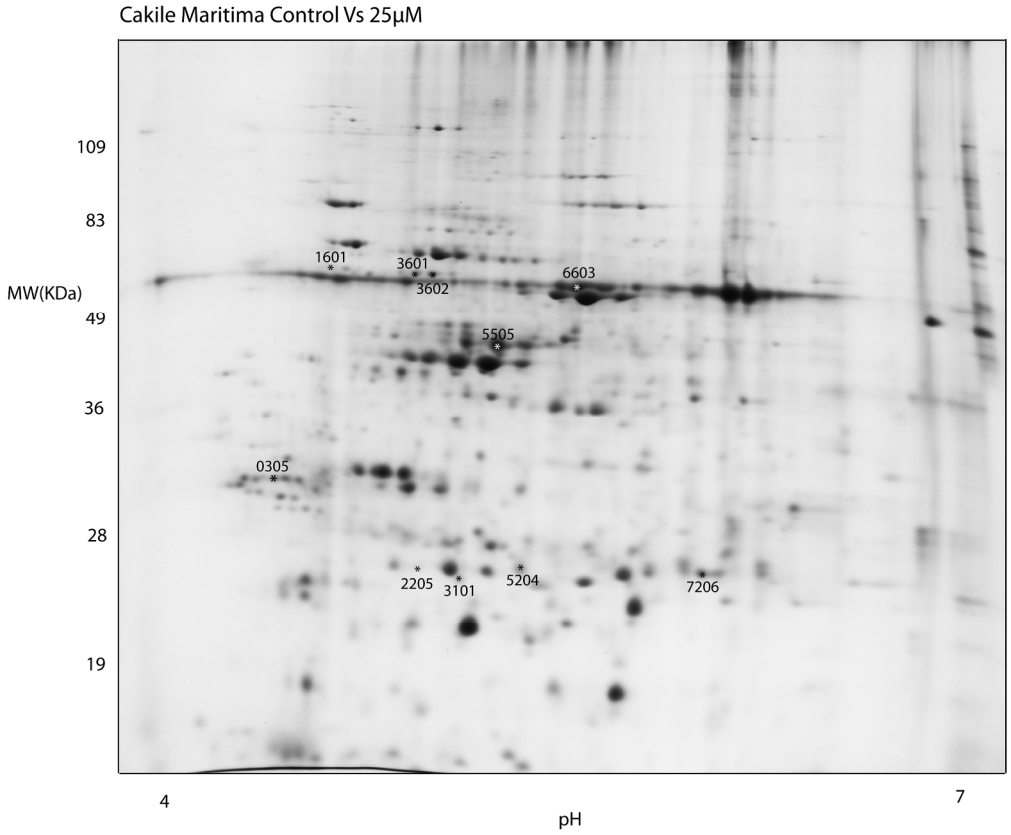

Figure 1A A representative gel from 2DE analysis of C. maritima leaves exposed to 25 µM CdCl2, in comparison to untreated controls.
219x181mm (300 x 300 DPI)

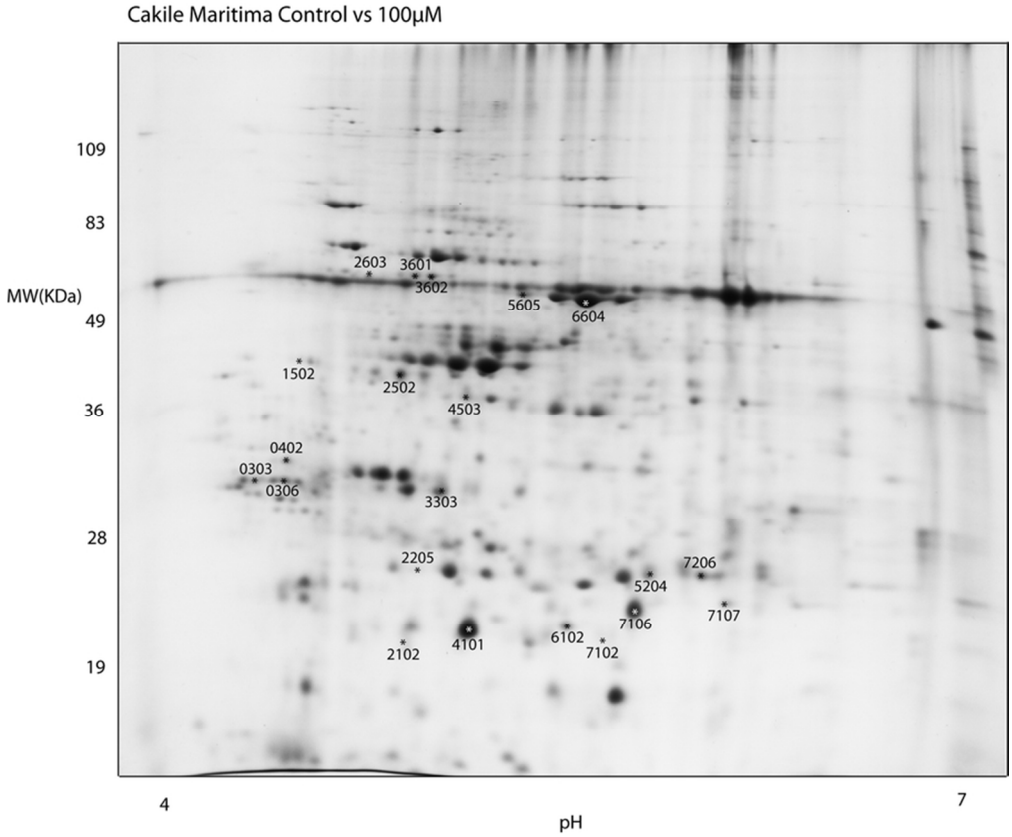

Figure 1B A representative gel from 2DE analysis of C. maritima leaves exposed to 100 µM CdCl2, in comparison to untreated controls.
76x63mm (300 x 300 DPI)

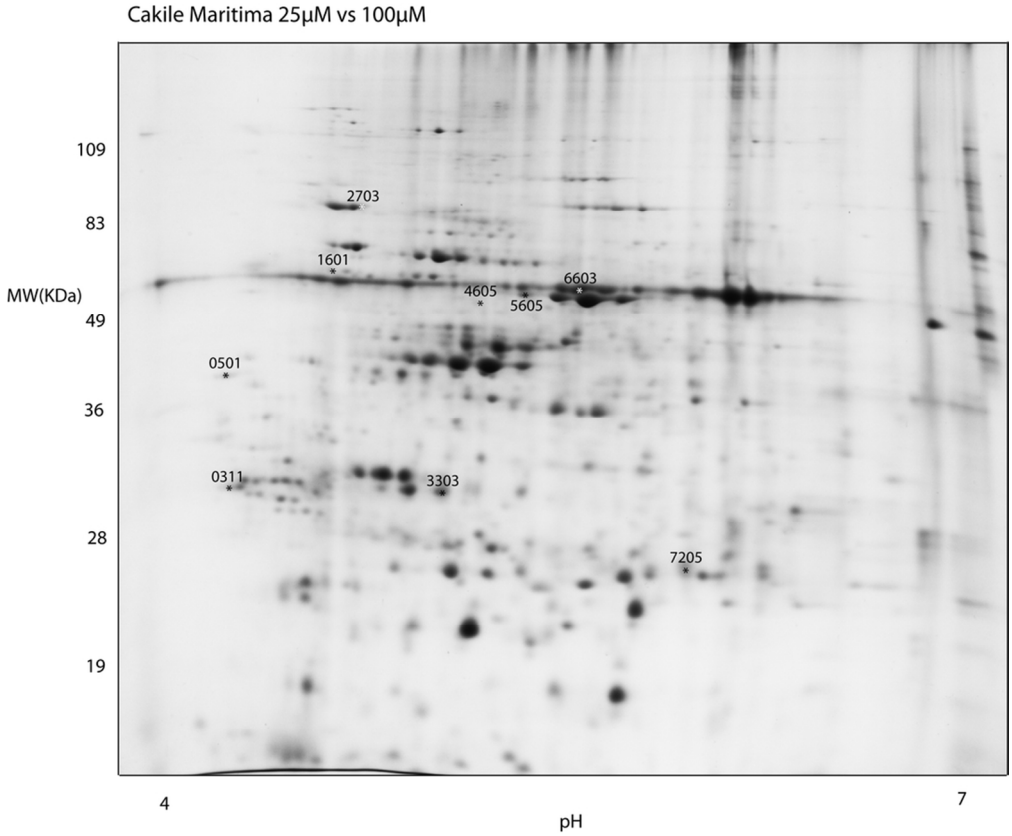

Figure 1C In C,are expressed spots differing between 25 µM and 100 µM gels.
90x75mm (300 x 300 DPI)

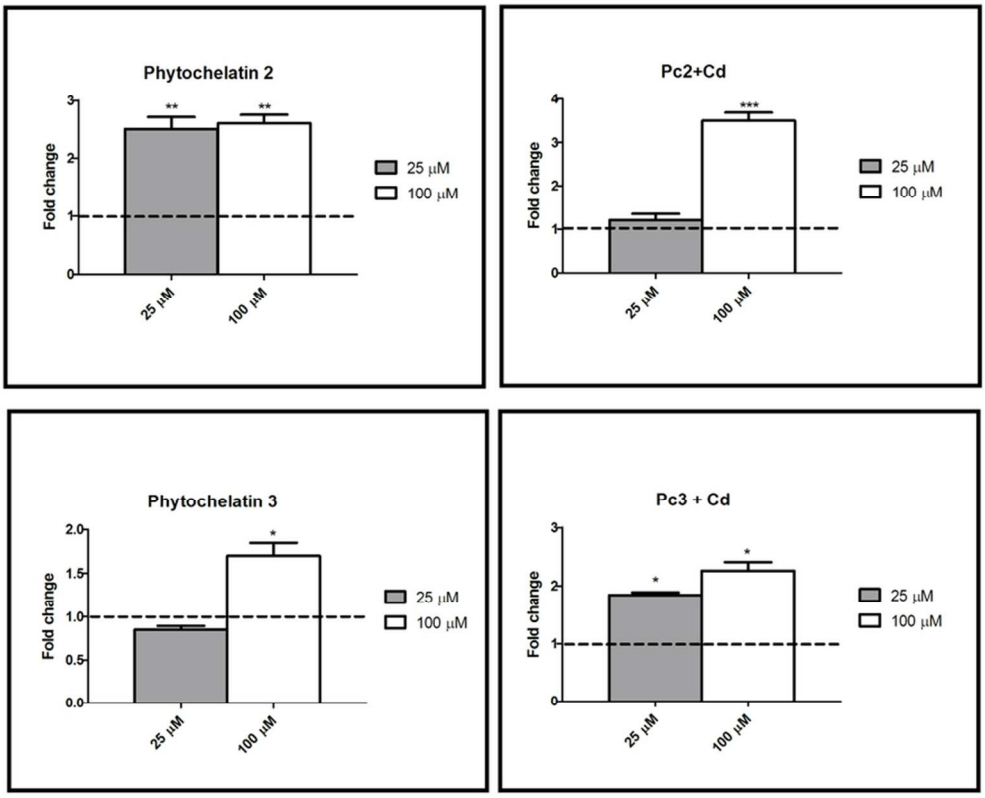

Figure 2 Variation in the levels of metabolites of the phytochelatins and relative cadmium adducts (A-D) in the leaves of Cakile maritima subjected to different Cd concentration, normalized against untreated controls (dashed line at 1 fold change, + SD calculated across normalized biological replicates of control leaves) . Measurements were performed in triplicate on pooled ground leaves coming from four individual plants per group (control, 25 and 100 µM).
* = $p<0.05$; ** = $p<0.01$ *** = $p<0.001$ ANOVA

75x61mm (300 x 300 DPI)

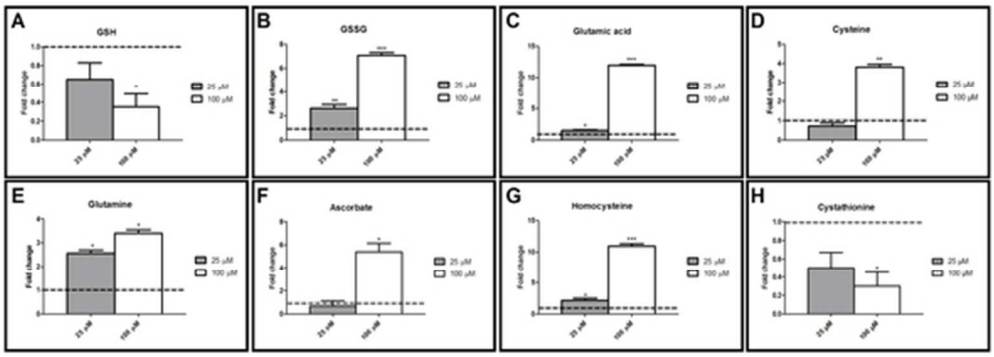

Figure 3 Variation in the levels of metabolites of the glutathione homeostasis (A-D), glutamine/glutamate metabolism (E), glutathione-ascorbate shuttle (F) and cysteine biosynthesis (G-H) in the leaves of Cakile maritima subjected to different Cd concentration, normalized against untreated controls (dashed line at 1 fold change, + SD calculated across normalized biological replicates of control leaves). Measurements were performed in triplicate on pooled ground leaves coming from four individual plants per group (control, 25 and 100 µM).
* = $p<0.05$; ** = $p<0.01$ *** = $p<0.001$ ANOVA

50x18mm (300 x 300 DPI)

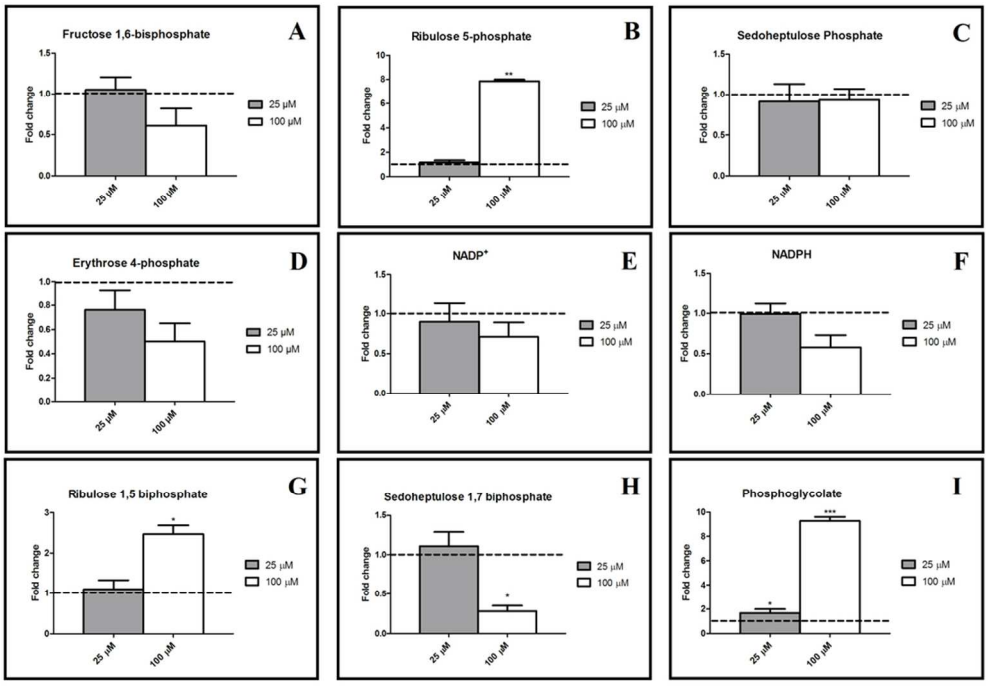

Figure 4 Variation in the levels of metabolic intermediates of the Pentose Phosphate Pathway (PPP) (A,B,C,D,E,F), Calvin cycle (C,D,G,H) and photorespiration (I) in the leaves of Cakile maritima subjected to different Cd concentration, normalized against untreated controls (dashed line at 1 fold change, + SD calculated across normalized biological replicates of control leaves) . Measurements were performed in triplicate on pooled ground leaves coming from four individual plants per group (control, 25 and 100 µM). * = $p<0.05$; ** = $p<0.01$ *** = $p<0.001$ ANOVA

94x65mm (300 x 300 DPI)

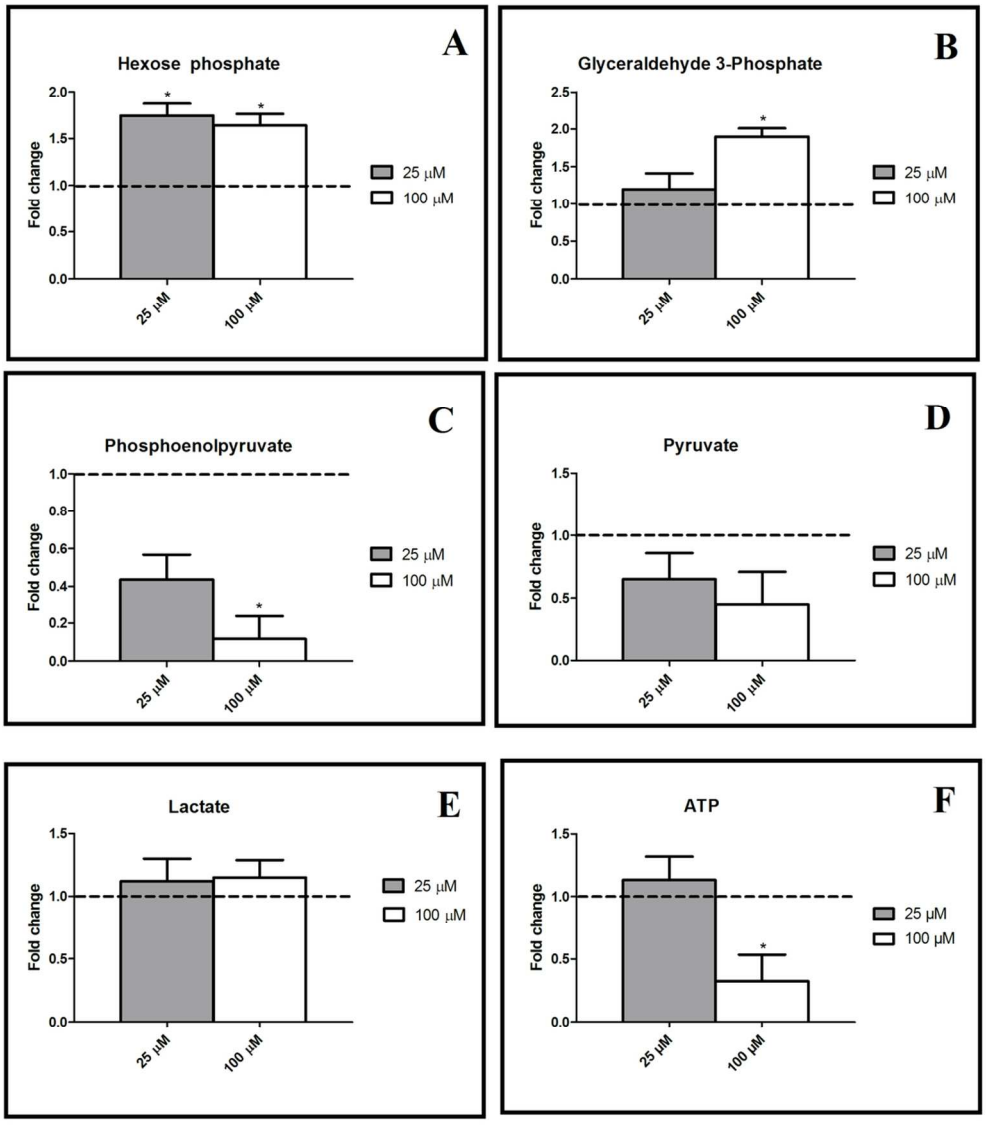

Figure 5 Variation in the levels of metabolites of glycolytic intermediates (A-E) and adenosine triphosphate (ATP) (F) in the leaves of Cakile maritima subjected to different Cd concentration, normalized against untreated controls (dashed line at 1 fold change, + SD calculated across normalized biological replicates of control leaves) . Measurements were performed in triplicate on pooled ground leaves coming from four individual plants per group (control, 25 and 100 µM).
* = p<0.05 ANOVA

105x119mm (300 x 300 DPI)

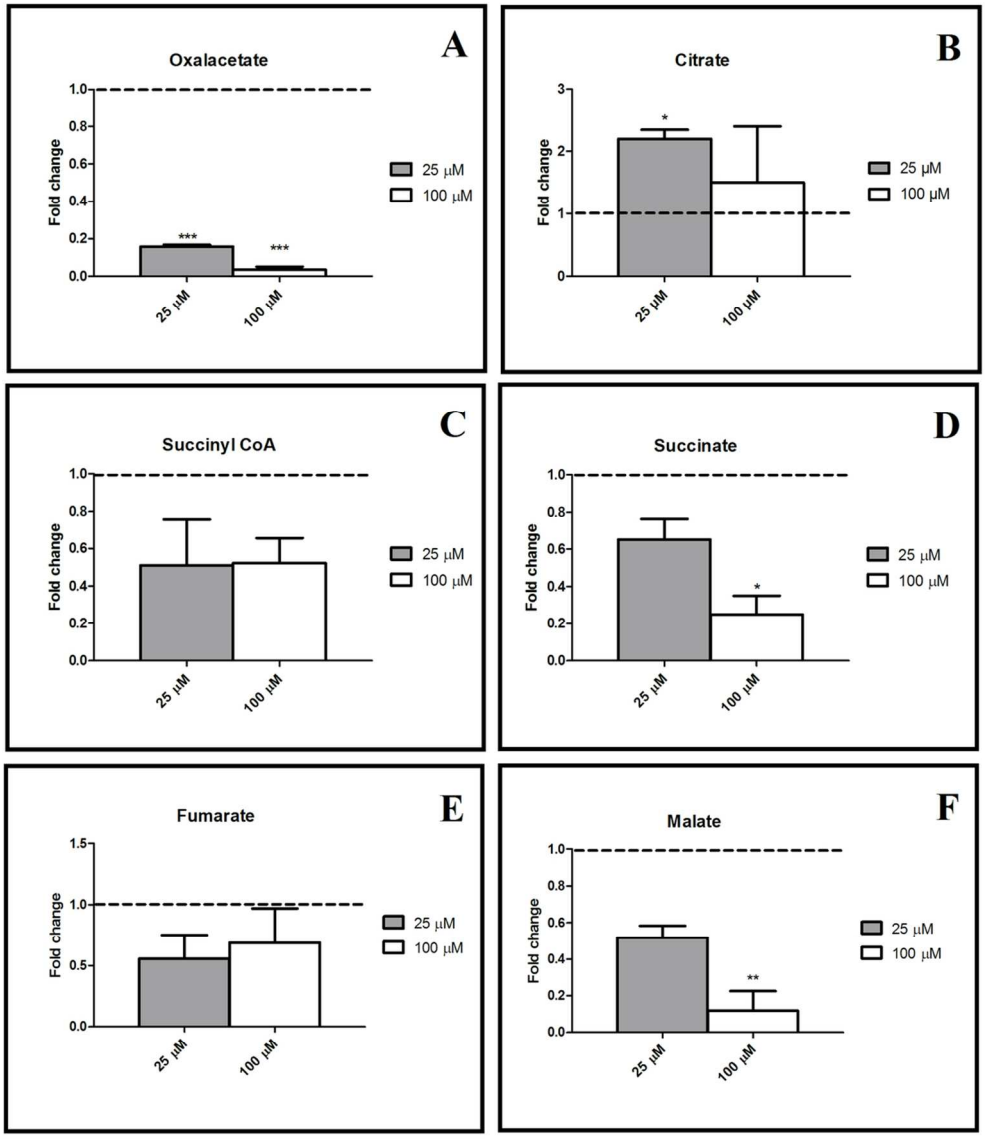

Figure 6 Variation in the levels of metabolites of organic acid of the tricarboxylic acid cycle (A-F) in the leaves of Cakile maritima subjected to different Cd concentration, normalized against untreated controls (dashed line at 1 fold change, + SD calculated across normalized biological replicates of control leaves) . Measurements were performed in triplicate on pooled ground leaves coming from four individual plants per group (control, 25 and 100 µM).
* = $p<0.05$; ** = $p<0.01$ *** = $p<0.001$ ANOVA

104x120mm (300 x 300 DPI)

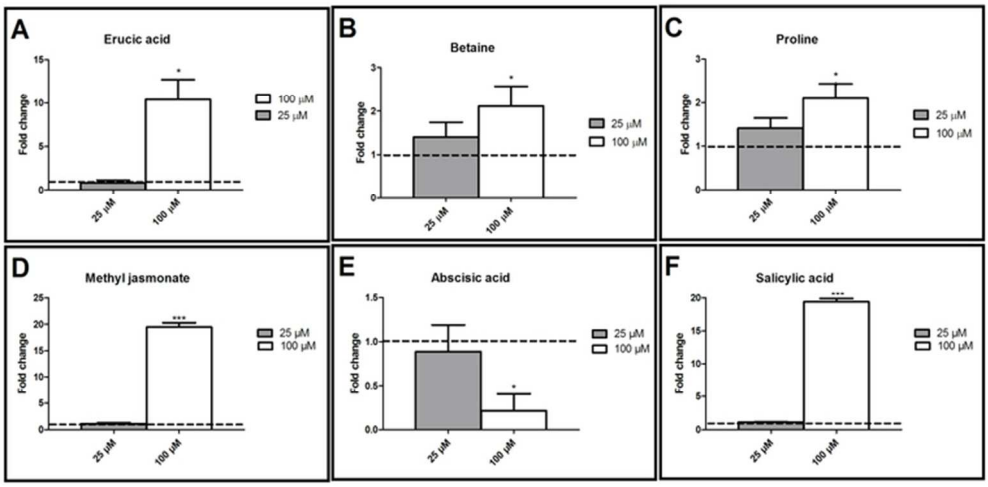

Figure 7 Variation in the levels of erucic acid (A - the main fatty acid component in C. maritima seed oil), the osmoprotectant betaine (B) and proline (C), and the plant hormones, methyl jasmonate (D), abscisic acid (E), and salicylic acid (F) in the leaves of Cakile maritima subjected to different Cd concentration, normalized against untreated controls (dashed line at 1 fold change, + SD calculated across normalized biological replicates of control leaves) . Measurements were performed in triplicate on pooled ground leaves coming from four individual plants per group (control, 25 and 100 µM).
* = $p<0.05$; *** = $p<0.001$ ANOVA

65x32mm (300 x 300 DPI)

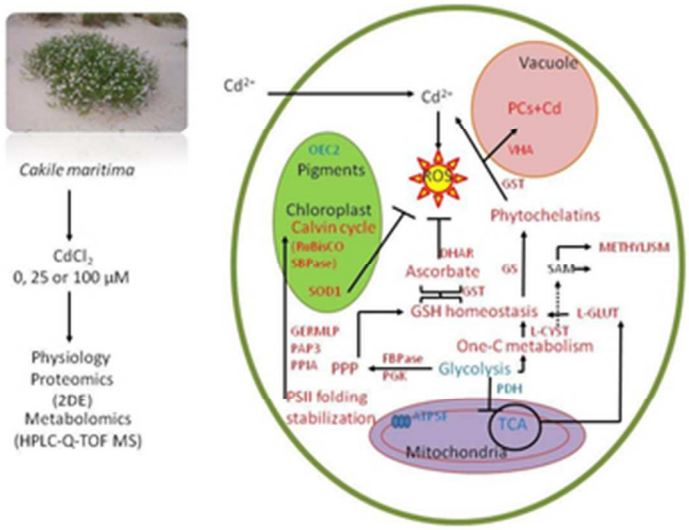

Figure 8 An overview of Cadmium stress responses in the halophyte Cakile maritima VHA:is a subunit of V-ATPase DHAR :Dehydro ascorbatereductase GST: Glutathione S-transferase. GERMLP: Germin like protein PAP3 PPIA Prolyl isomerase (also known as peptidylprolyl isomerase The picture of plant courtesy of Jürgen Howaldt

30x22mm (300 x 300 DPI)